FEBS Letters 580 (2006) 3161–3166

VHA-8, the E subunit of V-ATPase, is essential for pH homeostasis and larval development in *C. elegans*

Yon Ju Ji[a], Kyu Yeong Choi[a], Hyun-Ok Song[a], Byung-Jae Park[a], Jae-Ran Yu[b], Hiroaki Kagawa[c], Woo Keun Song[a], Joohong Ahnn[a,*]

[a] *Department of Life Science, Gwangju Institute of Science and Technology, Oryong 1, Puk-gu, Gwangju 500-712, South Korea*
[b] *Department of Parasitology, College of Medicine, Kon-Kuk University, Chungju 380-710, South Korea*
[c] *Graduate School of Natural Science and Technology, Okayama University, Okayama 700-8530, Japan*

Received 26 January 2006; revised 8 March 2006; accepted 24 April 2006

Available online 2 May 2006

Edited by Horst Feldmann

Abstract **Vacuolar H^+-ATPase (V-ATPase) is an ATP-dependent proton pump, which transports protons across the membrane. It is a multi-protein complex which is composed of at least 13 subunits. The *Caenorhabditis elegans vha-8* encodes the E subunit of V-ATPase which is expressed in the hypodermis, intestine and H-shaped excretory cells. VHA-8 is necessary for proper intestinal function likely through its role in cellular acidification of intestinal cells. The null mutants of *vha-8* show a larval lethal phenotype indicating that *vha-8* is an essential gene for larval development in *C. elegans*. Interestingly, characteristics of necrotic cell death were observed in the hypodermis and intestine of the arrested larvae suggesting that pH homeostasis via the E subunit of V-ATPase is required for the cell survival in *C. elegans*.**

Keywords: Vacuolar H^+-ATPase; Cell death; Necrosis; pH homeostasis; *C. elegans*

1. Introduction

The vacuolar H^+-ATPases (V-ATPases) belong to a family of ATP-dependent proton pumps that transport protons from the cytoplasmic compartment into the lumen of intracellular compartments or into the extracellular compartment [1,2]. The structure of V-ATPases is known to be similar to that of ATP synthases (or F-ATPase), which synthesize ATP using proton gradients in mitochondria, chloroplasts and bacteria [3–5]. The V-ATPases are composed of two domains: a peripheral V_1 domain and an integral V_0 domain [2,6,7]. The V_1 domain is composed of eight different subunits (subunits A–H) and is responsible for ATP hydrolysis. The V_0 domain is composed of five subunits (subunits a, d, c, c′ and c″) and is responsible for proton translocation. The *Caenorhabditis elegans vha-8* gene encodes the E subunit of the V_1 domain, which is thought to act as a peripheral stalk of the V-ATPase [8].

The V-ATPases have been reported to carry out various functions. They play an important role in receptor-mediated endocytosis: V-ATPases decrease pH in the early endosomes which is required for the dissociation of internalized ligand-receptor complexes to recycle receptors [1,2,6]. They also function in targeting of the newly synthesized lysosomal enzymes from the Golgi to lysosomes [2]. Moreover, V-ATPases are related to human disease. For example, the failure of urinary acidification by mutations in the B1 subunit gene of V-ATPase causes distal renal tubular acidosis, which is characterized by inappropriate alkaline urine [9,10]. Therefore, V-ATPases normally function to acidify the lumen of the kidney to make acidic urine. V-ATPases have also been implicated in osteopetrosis, which is a group of inherited diseases showing inadequate bone resorption due to osteoclast dysfunction. The human *TCIRG1* gene, which encodes an osteoclast-specific 116-kDa subunit of the V-ATPase, was reported to be mutated in osteopetrosis patients [11]. The implication of V-ATPase to osteopetrosis was further supported by the targeted disruption of *Atp6i*, encoding an osteoclast-specific V-ATPase subunit in mice [12].

In *C. elegans*, many genes encoding V-ATPase have been reported. For the V_0 domain, *vha-1*, *vha-2* and *vha-3* encode 16-kDa *c* subunits and *vha-4* encodes the 23-kDa *c″* subunit [13,14]. Particularly, four isoforms (*vha-5*, *vha-6*, *vha-7* and *unc-32*) of the *a* subunit were identified and these genes are expressed in a cell-specific manner [15]. For example, *vha-5* was expressed in the excretory cells, *vha-6* was expressed in intestine, *vha-7* was expressed in the hypodermis, and *unc-32* is expressed in nerve cells. For the V_1 domain, the C subunit is encoded by the *vha-11* which is required for ovulation and embryogenesis [16]. It has also been shown that the B subunit is encoded by the *vha-12* and the *vha-12* mutants suppressed necrosis in mechanosensory cell death due to improper cell acidification [17].

Previously, we had reported that *vha-8* encoding the E subunit of V-ATPase was mainly expressed in the H-shaped excretory cells and the apical plasma membrane of hypodermal cells [8]. RNAi targeted to the *vha-8* caused ovulation defects in the P_0 generations, and embryonic lethal phenotypes in the F_1 progeny. Moreover, animals treated with *vha-8* RNAi showed failure of yolk uptake by oocytes from the pseudoceolomic cavities indicating that V-ATPase functions in the receptor-mediated endocytosis in *C. elegans*. In this study, we characterize the role of VHA-8 in cellular acidification in *C. elegans*.

*Corresponding author. Fax: +82 62 970 2484.
E-mail address: joohong@gist.ac.kr (J. Ahnn).

Abbreviations: C. elegans, *Caenorhabditis elegans*; V-ATPase, vacuolar H^+-ATPase; GFP, green fluorescence protein; PCR, polymerase chain reaction

0014-5793/$32.00
doi:10.1016/j.febslet.2006.04.067

2. Materials and methods

2.1. C. elegans strains

The nematode *C. elegans* Bristol type (N2), DA768 *bli-6*(*sc16*) *egl-19*(*ad695*) *unc-24*(*e138*)*/nDf41 IV*, CB1282 *dpy-20*(*e1282*) *IV*, HE250 *unc-52*(*e699su250*) *II*, CB1370 *daf-2*(*e1370*) *III* were obtained from the *Caenorhabditis* Genetics Center at the University of Minnesota (St. Paul, MN). The KJ487 *vha-8*(*jh135*) *IV* mutants which were isolated in this experiment using reverse genetics method [18] were backcrossed at least six times. The genotype of *vha-8*(*jh135*) was determined by nested PCR using following primers; outer upstream primer 5′-ACAAACATCGACAAATATTCAAG-3′, outer downstream primer 5′-CTGACTTGTGGGACAATCTATAA-3′, inner upstream primer 5′-AAACTTGCAGAATCTACCGTATC-3′ and inner downstream primer 5′-CTTCTCGAAGAATTCCATAATCT-3′ and 5′-ATTACCTGGTTAGCAATAAGCTC-3′. Since *vha-8*(*jh135*) mutant was lethal, we maintained this mutant as a heterozygote [*vha-8*(*jh135*)*/bli-6*(*sc16*) *egl-19*(*ad695*) *unc-24*(*e138*) *IV*]. Worm breeding and handling were conducted as previously described [19].

2.2. Construction of GFP reporter plasmid

The cosmid C17H12 was obtained from Alan Coulson (The Sanger Center, UK). For pYJ37, the genomic DNA fragment containing 1.4 kb of 5′ upstream sequence and coding region of the *vha-8* gene was fused to a promoterless green fluorescence protein (GFP) vector, pPD95.75 (kindly provided by A. Fire) using the *Bam*HI and *Pst*I sites. For the nuclear GFP expression of intestinal and hypodermal cells, approximately 3.1 and 2.5 kb of the *vha-6* and the *vha-7* upstream fragment were amplified by polymerase chain reaction (PCR) using *C. elegans* lysate and inserted into pPD121.83 which is kindly provided by Dr. Andrew Fire. Microinjection of fusion plasmids and transformation marker pRF4 (dominant *rol-6*) was performed as described [20].

2.3. Analysis of nuclear fragmentation

We have generated stable transgenic lines which express GFP signal in the nuclei of the muscle, intestine and hypodermis. These transgenic lines were crossed into the *vha-8*(*jh135*)/+ heterozygote males. In the next generation, roller hermaphrodites which have the *vha-8*(*jh135*) mutation confirmed by PCR were selected and checked for GFP signals. *vha-8*(*jh135*)/+ heterozygotes transformed with GFP fusion constructs were successively genotyped by PCR, dead progeny containing the GFP signal which are scored as *vha-8*(*jh135*) homozygotes were selected and observed under the florescence microscope (Olympus BX50, Carl Zeiss Axio Imager A1).

2.4. Affinity purification of CeVHA-8 antibody and immunoflourescence

Rabbit anti-CeVHA-8 serum was affinity purified using CeVHA-8::GST fusion protein. The CeVHA-8 antibodies were allowed to bind to the CeVHA-8::GST proteins which were immobilized by glutathione sepharose™ 4B (Amersham Bioscience, 17-0756-01) and washed with 10 mM Tris (pH 8.0) more than three times. Approximately 500 μl of antibodies were successively eluted with 100 mM glycine (pH 3.0) into the tubes containing 50 μl of 1 M Tris (pH 8.0) to make the neutral pH. Wild-type worms were immunostained as previously described [21] with affinity purified CeVHA-8 antibodies.

2.5. RNA interference

The full-length *vha-8* cDNA and an *Eco*RI–*Xho*I fragment of 1.0-kb *vha-8* cDNA were cloned into an L4440 vector (kindly provided by A. Fire) for bacteria-mediated RNAi. Bacteria-mediated RNAi was conducted as previously described [22]. Twenty to thirty hermaphrodites of L4 or young adult stage were transferred onto plates seeded with *E. coli* HT115 (DE3) strain harboring L4440 plasmids containing *vha-8* full-length cDNA. After 12–24 h at 20 °C, P_0 worms were transferred onto new plates, and RNAi phenotypes in P_0 worms were observed. Bacteria transformed with L4440 vector containing *gfp* was used as a control.

2.6. Acridine orange staining

Acridine orange staining was slightly modified from a previously described method [16]. Adult worms were incubated for 30 min in staining buffer (40 μM acridine orange and 1% dimethyl sulfoxide) in the presence or absence of 25 μM bafilomycin A1 (Sigma). After washing with the phosphate buffer three times, animals were mounted and Nomarski images were obtained with a BX50 (Olympus) microscope. For fluorescence images, U-MWB2 fluorescence mirror unit (Olympus) was used.

3. Results

3.1. CeVHA-8 is expressed in the hypodermis, intestine and excretory cells

Previously, we had observed that *vha-8* was mainly expressed in the H-shaped excretory cells [8]. However, the genes encoding other subunits of V-ATPase in *C. elegans* have been reported to be also expressed in the intestine, pharynx, nerve ring, ventral nerve cord and hypodermis in addition to excretory cells [13–16]. Moreover, CeVHA-8 is the only putative E subunit of V-ATPase in *C. elegans* [8], indicating that CeVHA-8 might be expressed in other tissues or another protein may function instead of CeVHA-8. Therefore, we have further examined *vha-8* expression patterns extensively by GFP-tagging system and immunostaining. For the GFP-tagging

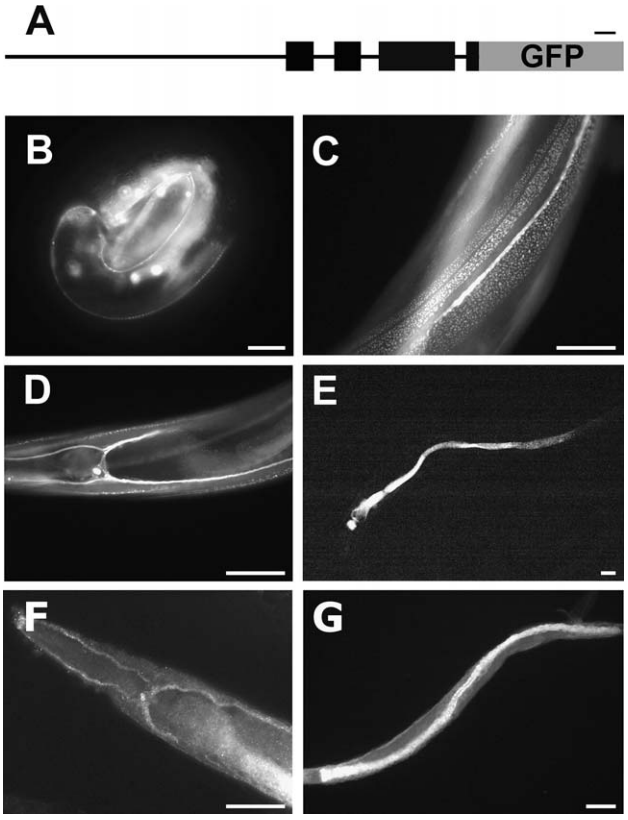

Fig. 1. Expression patterns of *vha-8* in *C. elegans*. (A) Approximately 1.4 kb 5′-upstream sequence of *vha-8* and the genomic DNA of *vha-8* gene were inserted into a gfp fusion vector (pPD95.75). The construct, pYJ37, was used for the analysis of GFP expression patterns. The scale bar indicates 100 bp. (B–E) GFP expression pattern of *vha-8*. (B) GFP signal began to be detected at the threefold stage embryo. GFP signal was detected in the hypodermis and intestine of the embryo. The scale bar indicates 5 μm. (C–E) Strong GFP signals were detected as punctuated patterns in the hypodermis (C), H-shaped excretory cells (D) and intestine (E) during larval and adult stages. The scale bars indicate 20 μm. (F and G) Immunofluoresence localization of VHA-8 in the wild-type *C. elegans*. Affinity purified VHA-8 antibodies detect VHA-8 protein in the H-shaped excretory cells (F) and intestine (G). The scale bars indicate 20 μm.

system, the translational fusion construct harboring the full-length *vha-8* coding region as well as the promotor region (Fig. 1A) was injected into wild-type animals. The GFP signal was first detected from the threefold stage of embryogenesis during development (Fig. 1B). At the threefold stage, GFP expression was observed in hypodermal and intestinal tissues. During larval and adult stages, GFP was strongly detected in the hypodermis (Fig. 1C) and intestine (Fig. 1E) as well as the excretory cells (Fig. 1D). Expression patterns of *vha-8* were further confirmed by immunostaining with affinity purified CeVHA-8 antibody. Antibody staining was detected in the H-shape excretory cells (Fig. 1F) and the intestine (Fig. 1G) which is consistent with the GFP expression pattern of *vha-8*.

3.2. CeVHA-8 is involved in cellular acidification and proper digestion in the intestine

It is known that V-ATPase regulates the pH homeostasis of cellular compartments in the eukaryotic cells [1,2], and proper acidification of these cellular compartments via V-ATPase was required for necrotic cell death of mechanosensory neurons in *C. elegans* [17]. In order to understand the role of CeVHA-8 in pH regulation, we stained *C. elegans* with acridine orange, a weak basic dye, which accumulates in acidic compartments. The acridine orange accumulated highly in the intestine of wild-type animals. This accumulation was blocked by bafilomycin A1, a specific inhibitor of V-ATPase, indicating that acidification of *C. elegans* intestine was likely achieved by the function of V-ATPase (Fig 2A and C). Moreover, adult animals of the P_0 generation treated with *vha-8* RNAi showed significantly less accumulation of acridine orange dye compared to that of wild type or animals treated with *gfp* RNAi (Fig 2D–F). This further confirmed that CeVHA-8 has a specific and critical role for the function of V-ATPase in the regulation of pH homeostasis in the *C. elegans* intestine.

In light of this function for CeVHA-8 in the intestine, we further examined the role of CeVHA-8 in the intestine. To observe the intestinal function, we used a GFP-expressing strain of OP50 bacteria which is the food source for *C. elegans* in the laboratory. We fed wild type animals with this GFP-expressing OP50 along with an RNase III deficient bacteria strain, HT115, which expresses *vha-8* double stranded RNA. In wild-type animals only treated with the GFP-expressing OP50, GFP was detected in the entire intestine, but weak near the most anterior intestinal ring (Figs. 2G and H), indicating that wild type worms exhibited normal digestion and absorption of GFP expressed by OP50. However, *vha-8* RNAi worms showed only strong GFP signals near the most anterior intestinal ring whereas most of the remaining intestine failed to show any GFP signal (Figs. 2I and J). Moreover, the anterior intestinal lumen of *vha-8* RNAi worms was enlarged, indicating that undigested GFP-expressing OP50 remained in the proximal region of the intestine of *vha-8* RNAi worms. Therefore, these digestive defects suggest that CeVHA-8 is required for the normal function of the intestine perhaps by regulating pH homeostasis.

3.3. A vha-8 deletion mutant, vha-8(jh135), was isolated in C. elegans

From our *vha-8* RNAi experiments, we realized that VHA-8 has an indispensable role in the early development of *C. elegans*, as RNAi treatment resulted in early embryonic lethality in the F_1 generation [8]. In order to further investigate functions of the *vha-8* gene, we isolated a *vha-8* deletion mutant, *vha-8*(*jh135*), by a PCR-based screening of 4,5′,8-trimethylpsoralen-ultraviolet mutagenized library. The deletion removed approximately 1.6 kb of the *vha-8* gene from the 5′ upstream region to the third exon (Figs. 3A and B). The deletion region was further confirmed by nested PCR using an inner primer that produced no PCR band in the *vha-8*(*jh135*) homozygous mutant but detected a 1.4 kb band in a wild type or *vha-8*(*jh135*) heterozygous animals (Fig. 3B).

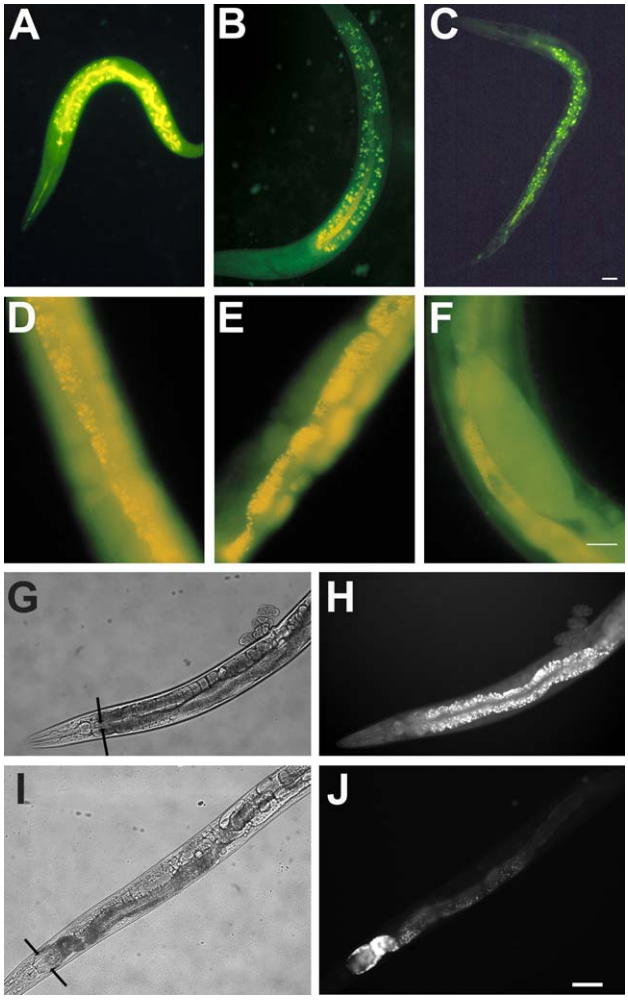

Fig. 2. CeVHA-8 functions in the intestine. (A–D) Acridine orange staining of *vha-8*(*jh135*) mutants or *vha-8* RNAi treated animals. The larval stage of wild-type animals (A), *vha-8*(*jh135*) mutants (B), wild-type animals treated with bafilomycin A1, a specific inhibitor of V-ATPase (C), adult stage wild-type animals (D), the *gfp*-targeted RNAi animal (E), and the *vha-8* targeted RNAi animal (F) were stained with acridine orange, a weak basic dye, which is accumulated into the acidic compartments. The acridine orange was highly accumulated in the intestine of wild-type animals (A,D) and the *gfp*-targeted RNAi animals (E), but not in the *vha-8*(*jh135*) mutants (B), *vha-8*-targeted RNAi animals (F) and the bafilomycin A1 treated wild-type animals (C). (G–J) Intestinal defects in the *vha-8* RNAi worm. (G and H) Wild type worms fed on GFP expressing OP50. (H) shows evenly distributed GFP signals in the entire intestine, but decreased GFP signals in the most anterior intestinal ring. (G) Normarski image of (H) and arrows indicate the width of intestinal lumen. (I and J) *vha-8* RNAi worm fed on the GFP-expressing OP50. (J) shows the concentrated GFP signals in the anterior region of the intestine. (I) Nomarski image of (J), and arrows indicate the width of the intestinal lumen which is appeared to be enlarged compared to the wild type. The scale bars indicate 20 μm.

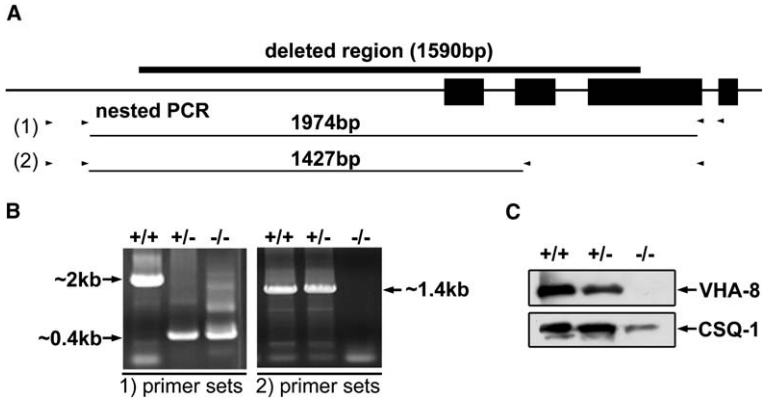

Fig. 3. Isolation of *vha-8*(*jh135*) mutants. (A) The *vha-8* gene contains four exons as shown by black boxes, and the thick horizontal bar indicates a deletion region which removes the 5′-upstream region and three exons of the *vha-8* gene. (1) and (2) indicate the primer sets (shown by arrowheads) used for genotyping the *vha-8*(*jh135*) mutations by nested PCR. (B) The amplified DNA fragments obtained from a single worm PCR, wild type (+/+), heterozygote (+/−) and homozygote (−/−), by using the primer sets described in A. Since homozygote (−/−) animals die at larval stage, we prepared lysate using a single dead larva as a template for PCR. In case of wild type (+/+) and heterozygote (+/−) lysates, we prepared using adult worms for the PCR. Absence of amplified DNA fragment in the (−/−) lane of 2) primer sets confirms that the worm is a homozygote. (C) Western blot analysis using VHA-8 anti-serum. We collected about 200 dead larvae for protein preparation of homozygote (−/−). In case of wild type (+/+) and heteozygote (+/−), we collected about 100 adult worms for protein preparation. No VHA-8 protein was detected in the *vha-8*(*jh135*) homozygote sample. In contrast, CSQ-1 protein (calsequestrin as a positive internal control) was detected from the same lysate, indicating that *vha-8*(*jh135*) is a functionally null mutant.

When Western blot analysis was performed, the anti-VHA-8 serum detected a single band of 29 kDa from protein extracts of a mixed stage population of wild-type and *vha-8*(*jh135*) heterozygous animals (Fig. 3C). However, no protein band was detected by anti-VHA-8 serum from *vha-8*(*jh135*) homozygotes, indicating that these deletion mutants are functionally null (Fig. 3C). The control anti-CSQ-1 serum detected a single band of 64 kDa from the same protein extract of *vha-8*(*jh135*) homozygotes.

3.4. *vha-8(jh135) mutants show larval lethality and necrotic cell death*

We characterized homozygote *vha-8*(*jh135*) mutants for their phenotypes. *vha-8*(*jh135*)/*dpy-13*(*e184*) *unc-22m52 IV* heterozygotes produced approximately 24% dead larva, indicating that *vha-8*(*jh135*) homozygotes might be larval lethal (Table 1). Moreover, PCR from single dead larvae using the primer within the deletion region produced no band, indicating that *vha-8*(*jh135*) homozygotes are larval lethal (Fig. 3B). Interestingly, *vha-8* mutants survived significantly longer than the embryonic lethality observed in *vha-8* RNAi-treated progeny. This is likely a result of a maternal requirement for *vha-8* in the early embryo. Indeed, the *vha-8* RNAi-treated P_0 generation showed defects in ovulation and yolk protein uptake [8].

We also performed acridine orange staining on the L1 *vha-8*(*jh135*) mutant larvae to further confirm a role for CeVHA-8 in cellular acidification. As expected, acridine orange failed to accumulate in the intestine of *vha-8*(*jh135*) mutants when compared to that of the wild-type animals, although a small accumulation was found in the proximal region of the intestine (Fig. 2B).

Strikingly, the *vha-8*(*jh135*) homozygotes began to arrest at L1 stage exhibiting swollen vacuoles in the hypodermis of the head region (Fig. 4B), and then the swollen vacuoles gradually spread throughout the whole body. Finally, pharyngeal pumping ceases at L2 stages with many vacuoles covering the entire body (Fig. 4C).

These swollen vacuoles are reminiscent to those of wild-type animals treated with hypoxia [23]. In *C. elegans*, hypoxia has been reported to cause a necrotic cell death whose characteristics are swollen necrotic cells and nuclear fragmentation shown by nuclear localized GFP signals. In order to test whether the *vha-8*(*jh135*) mutation also results in necrotic cell death, nuclear localized GFP under the control of the *myo-3* promoter was expressed in *vha-8*(*jh135*) mutants. The nuclear localized GFP were found to be fragmented in *vha-8*(*jh135*) mutants, whereas nuclei in wild-type were round and appeared to be intact (Figs. 4D and E), indicating that necrotic cell death is occurring in the larva of *vha-8*(*jh135*) mutants.

Because CeVHA-8 is expressed in the hypodermis, intestine and excretory cells, we have further examined whether nuclear fragmentation indicating necrotic cell death was also occurring in the hypodermis and intestine by using nuclear localized GFP. In order to express GFP in the nuclei of the hypodermal and intestinal cells, *vha-6* (for intestinal nuclei expression) and *vha-7* (for hypodermal nuclei expression) upstream sequences were cloned into the plasmid pPD121.83 which is a promoterless vector containing four repeated nuclear localized signals and *gfp* gene [15]. These constructs were injected into wild-type and *vha-8*(*jh135*) mutants.

C. elegans intestine is composed of nine intestinal rings (I–IX int ring) which are made of 20 intestinal cells. Each intestinal ring is composed of two intestinal cells except the most anterior intestinal ring which are made of four intestinal cells. In Fig. 4G, 19 nuclei of the intestinal cells are clearly shown in wild type larvae. The most anterior nucleus of intestinal ring is out of focus, so the two nuclei are juxtaposed in this figure.

Table 1
The lethality of *vha-8* mutant

Genotype of P_0	Lethality (%)[a]	n[b]
vha-8(*jh135*)/*dpy-13*(*e184*) *unc-22*(*m52*)	24.1 ± 7.8	1775
dpy-13(*e184*) *unc-22*(*m52*)	2.6 ± 3.6	1500

[a]Percentages of dead larva among total progenies.
[b]n indicates the numbers of progenies which we examined.

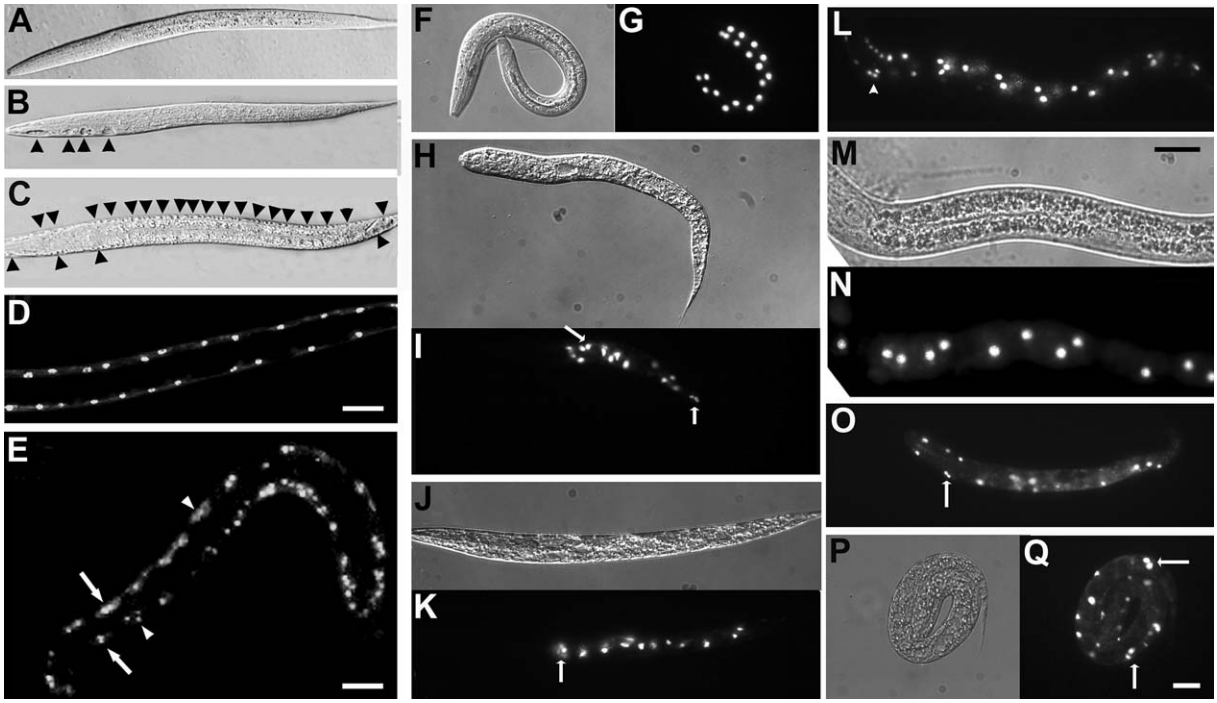

Fig. 4. The larval lethal phenotype of *vha-8*(*jh135*) mutants. (A–C) Nomarski images of L1 larvae of wild type (A) and *vha-8*(*jh135*) mutants (B and C). *vha-8*(*jh135*) mutants show swollen vacuoles (indicated by arrowheads) and die at the L1 stage. In the process of dying, the number of swollen vacuoles are increased and spread over the whole body. (D) Wild-type animals showing intact and round shaped nuclear-GFP in body-wall muscle cells, which was expressed by *pmyo-3::gfp* reporter. In contrast, the *vha-8*(*jh135*) mutants (E) showing fragmented GFP signal in the nuclei of the muscle cells (arrows and arrowheads). The F, H, J, M and P are the nomarski images of the G, I, K, N and Q, respectively. Wild-type *C. elegans* (G) shows round and intact nuclei of the 19 intestinal cells and the nuclei of the most anterior intestinal ring (Int I) is slightly out of focus and juxtaposed to the next nuclei. *vha-8*(*jh135*) mutants (I and K) show the fragmented nuclei (indicated by the arrows in I and K) in the intestinal cells, and the shapes of nuclei are irregular. Moreover, the numbers of nuclei are decreased in the *vha-8*(*jh135*) mutants compared to the wild-type, indicating that nuclei might have been already degraded in the *vha-8*(*jh135*) mutants. The entire body of L1 stage wild type worm (L) shows large numbers of hypodermal nuclei. The arrowhead in (L) indicates Hyp5, Hyp 6 and H0 cell nuclei, which are very closely located to each other between the two pharyngeal bulbs. The M and N show close-up images of wild type larvae from the posterior pharyngeal bulb to the mid-body. All the nuclei in (N) are round and intact. In contrast, the *vha-8*(*jh135*) mutants (O and Q) show the fragmented nuclei (arrows) and decreased number of nuclei in hypodermis. All the scale bars indicate 10 μm.

Compared to wild type worm which shows round and intact nuclei in the intestine, *vha-8*(*jh135*) mutants show fragmented and irregular nuclei (arrows in Figs. 4I and K), indicating that necrotic cell death is indeed occurring in the intestine.

In hypodermis, many cells are observed at L1 stage of wild type animal as shown in Fig. 4L with overlapping focal planes. The arrowhead indicates the Hyp5, Hyp6 and H0, which are very closely located to each other between two pharyngeal bulbs. As shown in close-up images of L1 wild type larvae from the posterior pharyngeal bulb to the mid-body (Figs. 4M and N), all the nuclei were round and intact. However, many nuclei of *vha-8*(*jh135*) mutant nuclei shown in Figs. 4O and Q were degraded, irregular and fragmented. The arrows indicate fragmented nuclei at the posterior pharyngeal bulb (O) and posterior body (Q) of *vha-8*(*jh135*) mutants, suggesting that necrotic cell death has occurred in the hypodermal cells as well. Thus, disruption of cytoplasmic pH via defected V-ATPase may cause the necrotic cell death in *C. elegans.*

4. Discussion

V-ATPases are known to regulate both intracellular as well as extracellular pH. Mutation in V-ATPase subunits lead to dysfunction at several levels in the organism. In this study we have shown that disruption of the E-subunit of V-ATPase, VHA-8, leads to defects in pH homeostasis in *C. elegans* in several tissues including the intestine. Moreover, we employed a novel approach using GFP-tagged bacteria to detect digestion/absorption defects in the intestine of these animals. Though the exact reason for the intestinal dysfunction is not known, we speculate that improper acidification may be playing a role. In mammals, mutations in an osteoclast-specific V-ATPase result in bone resorption defects which exhibit characteristic of the human disease osteopetrosis. These defects are due to improper extracellular acidification resulting from disruption of the V-ATPase. Further study of the nematode intestinal defects will determine whether this could be a genetic model for the debilitation human disease.

We also observed larval lethality in *vha-8*(*jh135*) mutants, as well as nuclear fragmentation and swollen vacuoles which are characteristic of necrotic cell death. In *C. elegans*, several cases of necrotic cell death have been reported. For instance, gain-of-function mutations in *mec-4* and *deg-1* genes are well known causes of the necrosis-like cell death in mechanosensory neurons [24,25]. Necrotic cell deaths in *mec-4*(*u231*) and *deg-1*(*u506*) mutants were shown to be suppressed by reduced aspartyl protease activity in *unc-52*(*e669su250*) genetic background, indicating that specific aspartyl proteases are required for necrotic cell death [26]. Another cause of necrotic cell-death

is hypoxia in *C. elegans*, which is suppressed by the specific loss-of-function allele *daf-2*(*e1370*), which encodes an insulin/insulin-like growth factor (IGF) receptor homolog gene [23].

To examine whether larval lethality could be a result of necrotic cell death caused by disruption of V-ATPase, we generated and observed *unc-52*(*e669su250*)*II;vha-8*(*jh135*)*IV* and *daf-2*(*e1370*)*III*;*vha-8*(*jh135*)*IV* double mutants. However, the lethality of *unc-52*(*e669su250*) *II*;*vha-8*(*jh135*) *IV* and *daf-2*(*e1370*) *III*;*vha-8*(*jh135*) *IV* double mutants were similar with *vha-8*(*jh135*) mutants alone (data not shown). This indicated that larval lethality in *vha-8*(*jh135*) mutants is independent of the reduced aspartic protease activity in *unc-52*(*e699su250*) mutants or loss-of-function allele of *daf-2*(*e1370*) mutants in *C. elegans*, and may suggest that necrotic cell death is a result of accumulated severe defects in the dying *vha-8*(*j135*) larvae. Therefore, further investigation is needed to reveal the essential role of CeVHA-8 in the larval development.

Recently, it was reported that cytoplasmic acidification by V-ATPase was required in necrotic cells, indicating that V-ATPase is required for necrotic cell death [17]. Specifically, knockdown of *vha-12* encoding a B subunit of V-ATPase suppressed necrotic cell death by increasing pH. However, *vha-8* mutants showed necrotic cell death in several tissues such as intestine, hypodermis and muscle which is not consistent with the suppression of necrotic cell death in neuronal cells by the knock-down of *vha-12*. A possible explanation could be that V-ATPase function of acidification of sub-celluar organelles may be required for specific neuronal degeneration, but general necrosis in other tissues such as intestine, hypodermis and muscle may be also caused by the failure of the proper cellular acidification due to the complete lack of functional V-ATPase.

Acknowledgements: The authors thank Dr. Alan Coulson for the C17H12 cosmid clone, Dr. Andy Fire for the GFP expression vector and L4440 plasmid (vector for bacteria-mediated RNA interference), and Dr. Yuji Kohara for the *C. elegans* cDNA library. Some *C. elegans* strains used in this work were obtained from the Caenorhabditis Genetics Center. This work was supported by the Korean Research Foundation Grant (KRF-2004-042-C00105).

References

[1] Nishi, T. and Forgac, M. (2002) The vacuolar (H+)-ATPases-nature's most versatile proton pumps. Nat. Rev. Mol. Cell Biol. 3, 94–103.
[2] Stevens, T.H. and Forgac, M. (1997) Structure, function and regulation of the vacuolar (H+)-ATPase. Annu. Rev. Cell Dev. Biol. 13, 779–808.
[3] Cross, R.L. (2000) The rotary binding change mechanism of ATP synthases. Biochim. Biophys. Acta 1458, 270–275.
[4] Weber, J. and Senior, A.E. (2000) ATP synthase: what we know about ATP hydrolysis and what we do not know about ATP synthesis. Biochim. Biophys. Acta 1458, 300–309.
[5] Fillingame, R.H., Jiang, W. and Dmitriev, O.Y. (2000) Coupling H^+ transport to rotary catalysis in F-type ATP synthases. J. Exp. Biol. 203, 9–17.
[6] Forgac, M. (1999) Structure and properties of the vacuolar (H^+)-ATPases. J. Biol. Chem. 274, 12951–12954.
[7] Bowman, E.J. and Bowman, B.J. (2000) Cellular role of the V-ATPases in Neurospora crassa. J. Exp. Biol. 203, 97–106.
[8] Choi, K.Y., Ji, Y.J., Dhakal, B.K., Yu, J.R., Cho, C., Song, W.K. and Ahnn, J. (2003) Vacuolar-type H+-ATPase E subunit is required for embryogenesis and yolk transfer in *Caenorhabditis elegans*. Gene 311, 13–23.
[9] Brown, D. and Breton, S. (2000) H^+V-ATPase dependent lumenal acidification in the kidney collecting duct and the epididymis/vas deferens. J. Exp. Biol. 203, 137–145.
[10] Karet, F.E., Finberg, K.E., Nelson, R.D., Nayir, A., Mocan, H., Sanjad, S.A., Rodriguez-Soriano, J., Santos, F., Cremers, C.W., Di Pietro, A., Hoffbrand, B.I., Winiarski, J., Bakkaloglu, A., Ozen, S., Dusunsel, R., Goodyer, P., Hulton, S.A., Wu, D.K., Skvorak, A.B., Morton, C.C., Cunningham, M.J., Jha, V. and Lifton, R.P. (1999) Mutations in the gene encoding B1 subunit of H^+-ATPase cause renal tubular acidosis with sensorineural deafness. Nature Genet. 21, 84–90.
[11] Frattini, A., Orchard, P.J., Sobacchi, C., Giliani, S., Abinun, M., Mattsson, J.P., Keeling, D.J., Andersson, A.K., Wallbrandt, P., Zecca, L., Notarangelo, L.D., Vezzoni, P. and Villa, A. (2000) Defects in TCIRG1 subunit of the vacuolar proton pump are responsible for a subset of human autosomal recessive osteopetrosis. Nature Genet. 25, 343–346.
[12] Li, Y.P., Chen, W., Liang, Y., Li, E. and Stashenko, P. (1999) Atp6i-deficient mice exhibit severe osteopetrosis due to loss of osteoclast-mediated extracellular acidification. Nature Genet. 23, 447–451.
[13] Oka, T., Yamamoto, R. and Futai, M. (1997) Three vha genes encode proteolipids of *Caenorhabditis elegans* vacuolar-type ATPase. J. Biol. Chem. 272, 24387–24392.
[14] Oka, T., Yamamoto, R. and Futai, M. (1998) Mutiple genes for vacuolar-type ATPase proteolipids in *Caenorhabditis elegans*. J. Biol. Chem. 273, 22570–22576.
[15] Oka, T., Toyomura, T., Honjo, K., Wada, Y. and Futai, M. (2001) Four subunit a isoforms of *Caenorhabditis elegans* Vacuolar H+-ATPase. J. Biol. Chem. 276, 33079–33085.
[16] Oka, T. and Futai, M. (2000) Requirement of V-ATPase for ovulation and embryogenesis in *Caenorhabditis elegans*. J. Biol. Chem. 275, 29556–29561.
[17] Syntichaki, P., Samara, C. and Tavernarakis, N. (2005) The Vacuolar H+-ATPase mediates intracellular acidification required for neurodegeneration in *C. elegans*. Curr. Biol. 15, 1249–1254.
[18] Park, B.J., Lee, D.G., Yu, J.R., Jung, S.K., Choi, K., Lee, J., Lee, J., Kim, Y.S., Lee, J.I., Kwon, J.Y., Lee, J., Singson, A., Song, W.K., Eom, S.H., Park, C.S., Kim, D.H., Bandyopadhyay, J. and Ahnn, J. (2001) Calreticulin, a calcium-binding molecular chaperone, is required for stress response and fertility in *Caenorhabditis elegans*. Mol. Biol. Cell. 12, 2835–2845.
[19] Brenner, S. (1974) The genetics of *Caenorhabditis elegans*. Genetics 77, 71–94.
[20] Mello, C. and Fire, A. (1995) DNA transformation. Methods Cell Biol. 48, 451–482.
[21] Ahnn, J. and Fire, A. (1994) A screening for genetic loci required for body wall muscle development during embryogenesis *in Caenorhabditis elegans*. Genetics 137, 438–498.
[22] Kamath, R.S., Martinez-Campos, M., Zipperlen, P., Fraser, A.G. and Ahringer, J. (2000) Effectiveness of specific RNA-mediated interference through ingested double-stranded RNA in *Caenorhabditis elegans*. Genome Biol. 2, RESEARCH0002.1-9.
[23] Scott, B.A., Avidan, M.S. and Crowder, C.M. (2002) Regulation of hypoxic death in *C. elegans* by the insulin/IGF receptor homolog DAF-2. Science 296, 2388–2391.
[24] Hall, D.H., Gu, G., Garcia-Anoveros, J., Gong, L., Chalfie, M. and Driscoll, M. (1997) Neuropathology of degenerative cell death in *Caenorhabditis elegans*. J. Neurosci. 17, 1033–1045.
[25] Driscoll, M. and Chalfie, M. (1991) The mec-4 gene is a member of a family of *Caenorhabditis elegans* genes that can mutate to induce neuronal degeneration. Nature 14, 588–593.
[26] Syntichaki, P., Xu, K., Driscoll, M. and Tavernarakis, N. (2002) Specific aspartyl and calpain proteases are required for neurodegeneration in *C. elegans*. Nature 31, 939–944.